

# Confirmation of ultrahigh-temperature metapelitic granulite in the Altay orogen and its geological significance

Laixi Tong · Yibing Chen · Linli Chen

Received: 10 November 2013 / Accepted: 8 March 2014 / Published online: 27 March 2014  
© Science China Press and Springer-Verlag Berlin Heidelberg 2014

**Abstract** Through petrography, mineral compositions and  $P$ - $T$  estimate results, an ultrahigh-temperature (UHT) metapelitic granulite has recently been identified from near Kalasu in the east of Altay city, with an assemblage  $gt$ - $opx$ - $sil$ - $cd$ - $sp$ - $bt$ - $pl$ - $qtz$ . The orthopyroxene has a high-Al feature, and its  $Al_2O_3$  content is as high as 8.7 wt%, indicating a UHT metamorphic condition. Its peak metamorphic condition is estimated as:  $P = \sim 0.80$  GPa,  $T = \sim 960$  °C. Metamorphic textural relations and  $P$ - $T$  estimate results show a post-peak near-isobaric cooling anticlockwise  $P$ - $T$  path. Zircon U-Pb age results ( $271 \pm 5$  Ma) support that the UHT metamorphic event in the region occurred in the Permian. The identification of the UHT metapelitic granulite from near Kalasu confirms the existence of the Permian UHT metamorphism in the Altay orogen, implying that the Permian extensional tectonic setting of a high-heat flow in the southern part of the Altay orogen may be closely associated with the Permian Tarim mantle plume activity.

**Keywords** Ultrahigh-temperature metamorphism · Metapelitic granulite · Altay orogen ·  $P$ - $T$  path

## 1 Introduction

In the last several years, the study of ultrahigh-temperature (UHT) metamorphism has become an important frontier research topic of the metamorphic-geological field after the ultrahigh-pressure metamorphic study. UHT metamorphism

is a type of very high temperature granulite facies metamorphism, where crustal rocks experienced peak metamorphic temperature in excess of 900 °C, generally characterized by indicative mineral assemblages such as orthopyroxene+sillimanite+quartz, sapphirine+quartz, and osunilite+quartz, while orthopyroxene shows a high-Al feature ( $Al_2O_3 > 8.0$  wt%) [1–3]. To date, there have been over 30 localities of UHT granulites reported from around the world, e.g. East Antarctica, India and North China, etc. [4–6]. As the UHT granulites contain important information on the processes of lower crust evolution and crust-mantle interaction, their study is critical to understanding the processes of lower crust evolution and crust-mantle interaction. In this paper, through petrography and  $P$ - $T$  estimate results, the existence of UHT metamorphism in the Altay orogenic belt is confirmed, with a construction of its  $P$ - $T$  evolution path. This provides an important constraint on understanding the evolutionary process of the Altay orogenic belt.

## 2 Geological background

The Altay orogenic belt belongs to an important part of the Central Asian Orogenic Belt, and it is also a typical Phanerozoic accretionary orogenic belt in the world [7–9]. This orogenic belt is located on the south-western margin of the Siberian plate, and its southern part is bounded by the large Erqis fault with the Junggar plate [10, 11]. The rocks in this belt record the tectonic processes of Neoproterozoic to late Paleozoic, with the extensive development of Paleozoic medium-low pressure grade metamorphic zones and gneissic thermal dome structures [12–15], and contains abundant mineral resources. The metamorphic zones can be divided into kyanite-type and andalusite-type, and show a main feature of greenschist-amphibolite facies metamorphism [13,

L. Tong (✉) · Y. Chen · L. Chen  
State Key Laboratory of Isotopic Geochemistry, Guangzhou  
Institute of Geochemistry, Chinese Academy of Sciences,  
Guangzhou 510640, China  
e-mail: lxtong@gig.ac.cn

[15], and locally granulite facies metamorphism [16–18]. The greenschist-amphibolite facies metamorphism was thought to have occurred in the late Devonian (~365 Ma) [11, 15], probably associated with the arc-continent collision during the early to middle Palaeozoic [11, 19]. Other researchers further consider that the low-pressure high-temperature metamorphism occurred in the period of 380–390 Ma, and was associated with the development of ridge-subduction and slab-window formation [20–22]. In addition, the granulite facies high-temperature metamorphism of this belt was considered to have occurred in the Permian (270–290 Ma) [17, 18], reflecting that the region experienced an important phase of high-grade structural metamorphic event in the late Palaeozoic [23, 24].

A large number of granitoids and orthogneisses occupy about 40 % of rocks in the orogenic belt, consisting mainly of early Palaeozoic syn-orogenic and late Palaeozoic post-orogenic granitic bodies, and may be subdivided into tonalite, granodiorite and biotite granite, with minor two mica granite [19]. The ages of the former are mainly between 370–450 Ma, with a geochemical signature of arc magmatism [19, 25], whereas the ages of the latter are between 270–280 Ma [26–29], with a mantle-derived signature [30]. Additionally, some mantle-derived mafic intrusive rocks and an ultramafic intrusive complex of about 280 Ma occur at Kalatongke and Wuqiagou in Fuyun County [31, 32]. These Permian ages are completely consistent with the timing of the large Erqis fault/shear zone [33].

In recent years, Wang et al. [18] recognized the medium-low-pressure high-temperature (~800 °C) metapelitic granulites near Dakalasu of Altay, and Li et al. [34] reported a UHT (>900 °C) metapelitic granulite assemblage from Wuqiagou in Fuyun County. These support that the Altay orogenic belt experienced high-temperature to UHT granulite facies metamorphism. However, up to the present, detailed studies still lack constraints on the metamorphic *P-T* evolutionary history, and different opinions also exist on their tectonic settings. For instance, Wang et al. [18] considered that the Permian medium-low-pressure high-temperature metamorphism in the Altay orogenic belt formed in an extensional tectonic setting, whereas Li et al. [34] thought that the UHT granulite metamorphism might be associated with an ancient oceanic crustal subduction and plate collision in the Altay region. In the present paper, a detailed petrographic study and *P-T* estimates are undertaken for the UHT metapelitic granulite and its mineral assemblages recently identified near Kalasu of Altay, with the construction of a *P-T* evolutionary path. Combined with available age data, the possible tectonic setting will also be discussed.

### 3 Petrographic features of the UHT metapelitic granulite

The UHT metapelitic granulite described in this paper is located near Kalasu in the southeast of Altay city, and is situated within the medium-low pressure pelitic granulite zone reported by Wang et al. [18] (Fig. 1). The UHT metapelitic granulite occurs as tectonic lenses within the medium-low pressure pelitic granulites and both of them generally experienced partial melting and migmatitization, the latter of which shows D1 folding and D2 shear structures. The major petrographic features are described in the following.

Electron microprobe data of major minerals in the UHT metapelitic granulite (Table 1) were obtained on a JXA-8100 microprobe machine at State Key Laboratory of Isotopic Geochemistry, Guangzhou Institute of Geochemistry, Chinese Academy of Sciences, with the following experiment conditions: accelerating voltage of 15 kV; beam current of  $3 \times 10^{-8}$  Å; beam width of 1 µm; and data correction by using a ZAF method.

The mineral assemblages in the UHT metapelitic granulite are: garnet (10 %), orthopyroxene (7 %–8 %), sillimanite (2 %–3 %), cordierite (10 %–12 %), spinel (4 %–5 %), biotite (15 %–20 %), plagioclase (15 %–20 %), quartz (20 %–25 %) and minor ilmenite and magnetite. No K-feldspar was observed. The petrographic observations show that the rock develops two phases of fabrics S1 and S2 (Fig. 2a), probably in response to D1 compressional deformation and D2 shear deformation in outcrop, respectively. Coarse-grained biotite, garnet, orthopyroxene, cordierite, plagioclase and quartz comprise an S1 foliation and peak M1 mineral assemblage. Garnet contains inclusions of ilmenite and biotite (Fig. 2a) as well as spinel and orthopyroxene (Fig. 2b), and cordierite also contains spinel and sillimanite inclusions (Fig. 2c). The aligned mineral assemblage opx-bt-sil-pl-qtz in the matrix indicates an S2 foliation and M2 mineral association (Fig. 2d). MgO content in the garnet core is higher than that of the rim, and they are 8.4 wt% and 6.7 wt%, respectively. Orthopyroxene inclusions contains a low Al<sub>2</sub>O<sub>3</sub> content of about 4.6 wt%, in response to an  $X_{Al}$  (=Al/2) value of 0.102. The Al<sub>2</sub>O<sub>3</sub> content in peak orthopyroxene is markedly higher than that of the inclusions and the second phase of orthopyroxene, whilst the orthopyroxene core has the highest Al<sub>2</sub>O<sub>3</sub> content of 8.7 wt%, remarkably higher than that of the rim (6.3 wt%), with corresponding  $X_{Al}$  values of 0.194 and 0.141, respectively. Cordierite has an Mg/(Fe<sup>2+</sup>+Mg) value of 0.855. Spinel inclusions have a lower ZnO content (1.4 wt%) than that of spinel in the matrix (2.3 wt%), with corresponding Mg/(Fe<sup>2+</sup>+Mg) values of 0.424 and 0.277, respectively. Biotite is brown in colour, and has a Mg/(Fe<sup>2+</sup>+Mg) value of 0.631, with a TiO<sub>2</sub> content as high as

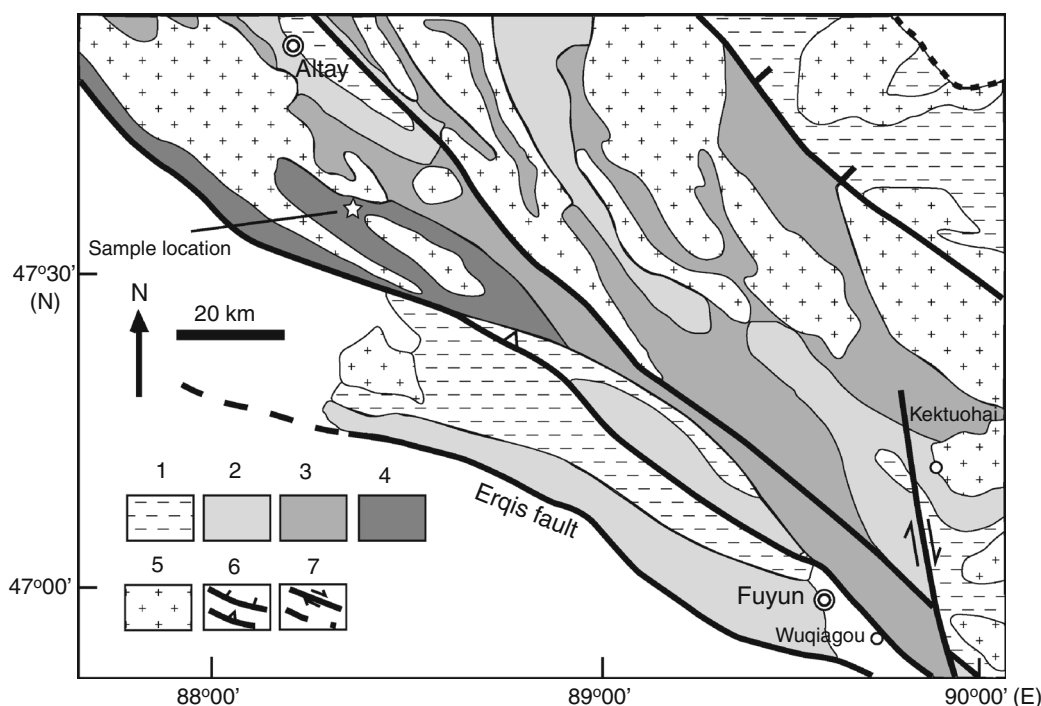


**Fig. 1** A simplified geological map of the Altay region (after Wang et al. [18]). 1 greenschist facies; 2 lower amphibolite facies; 3 upper amphibolite facies (sillimanite zone); 4 granulite facies; 5 granite; 6 normal fault and thrust fault; 7 strike-slip fault and inferred fault

4.6 wt%. Anorthite content in plagioclase is in a range of 31 %–46 %.

The textural relations and mineral compositions show that three-stage mineral assemblages can be distinguished in the UHT metapelitic granulite as follows: (1) pre-peak opx-sp-bearing or sp-sil-bearing inclusion assemblage (M0), characterized by low  $\text{Al}_2\text{O}_3$  contents (4 wt%–5 wt%) in orthopyroxene; (2) peak gt-opx-cd-bearing UHT mineral assemblage (M1), characterized by high  $\text{Al}_2\text{O}_3$  contents (8.7 wt%) in orthopyroxene; (3) post-peak opx-sil-bt-bearing high-temperature mineral assemblage (M2), with medium  $\text{Al}_2\text{O}_3$  contents (6 wt%–7 wt%) in orthopyroxene.

#### 4 Metamorphic conditions and $P$ - $T$ path

As many gt-opx thermobarometers fail to consider the effects of  $\text{Fe}^{2+}$ -Mg reset, which generally occurs between mineral pairs during the retrograde metamorphism after peak granulite facies metamorphism, these thermobarometers cannot give true peak or pre-peak  $P$ - $T$  conditions. Therefore, in this paper we adopt the gt-opx thermobarometer corrected by Pattison et al. [35] to estimate peak and pre-peak  $P$ - $T$  conditions of the UHT metapelitic granulite.

Low-Al orthopyroxene inclusions in garnet and the garnet in contact with the inclusions can be used to estimate  $P$ - $T$  conditions of pre-peak metamorphic stage (M0),

and the calculated results indicate that  $P$ - $T$  conditions of pre-peak metamorphic stage are  $\sim 0.7$  GPa/ $\sim 890$  °C. Garnet core compositions and equilibrated high-Al orthopyroxene compositions may reflect formation conditions of peak stage (M1), and the estimate results show that  $P$ - $T$  conditions of peak UHT metamorphic stage are  $\sim 0.8$  GPa/ $\sim 960$  °C. Because the post-peak opx-sil-bt-bearing high-temperature mineral assemblage (M2) does not contain garnet and the above gt-opx thermobarometer thus cannot be used to estimate its  $P$ - $T$  conditions, the average  $P$ - $T$  calculation method via Thermocalc may be utilised to estimate its formation conditions, and the results indicate that  $P$ - $T$  conditions of post-peak metamorphic stage (M2) are  $\sim 0.9$  GPa/ $\sim 870$  °C.

Thus, in the petrogenetic grid for the metapelites in the KFMASH model system [36], the above  $P$ - $T$  conditions of three different metamorphic stages define an anticlockwise  $P$ - $T$  path of initial prograde heating and increase in pressure and post-peak near isobaric cooling (Fig. 3).  $P$ - $T$  conditions of  $\sim 0.7$  GPa/ $\sim 890$  °C for pre-peak opx-sp-bearing and sp-sil-bearing inclusion assemblages (M0) are very close to and consistent with the medium-low pressure high-temperature stability field that contains sp-bearing assemblages in the petrogenetic grid. Whereas  $P$ - $T$  conditions of  $\sim 0.8$  GPa/ $\sim 960$  °C for peak UHT metamorphic stage (M1) are compatible with the high-Al feature ( $\text{Al}_2\text{O}_3 > 8.0$  wt%) in peak orthopyroxene indicating a UHT metamorphic condition ( $> 900$  °C).  $P$ - $T$  conditions of

**Table 1** Electron microprobe analyses of major minerals in the UHT metapelitic granulite

	gt(c)	gt(r)	opx(i)	opx(c)	opx(c)	opx(r)	opx(2)	sil	sp(i)	sp(o)	cd	bt	pl
SiO <sub>2</sub>	38.88	39.06	49.19	47.25	47.14	48.23	47.87	37.62	0.03	0.02	49.71	36.22	60.85
TiO <sub>2</sub>	0.07	0.06	0.03	0.00	0.08	0.04	0.05	0.02	0.04	0.00	0.06	4.57	0.01
Al <sub>2</sub> O <sub>3</sub>	22.02	21.6	4.59	8.73	8.65	6.29	6.84	60.94	59.14	57.44	33.96	16.60	24.35
Cr <sub>2</sub> O <sub>3</sub>	0.03	0.03	0.03	0.00	0.03	0.00	0.01	0.04	0.25	1.16	0.00	0.12	0.00
FeO	28.48	30.20	25.52	24.73	24.82	24.75	25.32	0.79	28.59	31.86	4.25	14.31	0.03
MnO	1.10	1.17	0.25	0.26	0.18	0.23	0.54	0.00	0.09	0.07	0.05	0.01	0.00
MgO	8.44	6.68	20.49	18.79	18.45	19.54	18.45	0.01	10.42	6.58	11.21	13.77	0.01
CaO	1.24	1.42	0.06	0.03	0.05	0.03	0.05	0.08	0.00	0.00	0.01	0.00	5.72
Na <sub>2</sub> O	0.00	0.01	0.00	0.00	0.01	0.00	0.02	0.00	0.08	0.14	0.09	0.22	8.74
K <sub>2</sub> O	0.00	0.00	0.00	0.00	0.00	0.00	0.00	0.00	0.00	0.01	0.00	10.14	0.16
ZnO									1.39	2.32			
Total	100.26	100.23	100.16	99.79	99.41	99.11	99.15	99.50	100.02	99.58	99.39	95.96	99.85
O	12	12	6	6	6	6	6	10	4	4	18	11	8
Si	3.000	3.040	1.842	1.775	1.781	1.825	1.820	2.047	0.001	0.001	4.962	2.692	2.711
Ti	0.004	0.004	0.001	0.000	0.002	0.001	0.001	0.001	0.001	0.000	0.005	0.255	0.000
Al	2.003	1.982	0.203	0.387	0.385	0.281	0.307	3.907	1.884	1.882	3.997	1.455	1.279
Cr	0.002	0.002	0.001	0.000	0.001	0.000	0.000	0.001	0.005	0.025	0.000	0.007	0.000
Fe <sup>3+</sup>	0.000	0.000	0.110	0.063	0.049	0.068	0.051	0.000	0.111	0.099	0.071	0.000	0.001
Fe <sup>2+</sup>	1.838	1.966	0.689	0.714	0.735	0.716	0.754	0.036	0.531	0.641	0.284	0.890	0.000
Mn	0.072	0.077	0.008	0.008	0.006	0.007	0.017	0.000	0.002	0.002	0.004	0.001	0.000
Mg	0.971	0.775	1.144	1.052	1.039	1.102	1.045	0.001	0.420	0.273	1.668	1.525	0.001
Ca	0.103	0.118	0.002	0.001	0.002	0.001	0.002	0.005	0.000	0.000	0.001	0.000	0.273
Na	0.000	0.002	0.000	0.000	0.001	0.000	0.001	0.000	0.004	0.008	0.017	0.032	0.755
K	0.000	0.000	0.000	0.000	0.000	0.000	0.000	0.000	0.000	0.000	0.000	0.962	0.009
Zn									0.040	0.069			
Sum	7.993	7.965	4	4	4	4	4	5.998	3	3	11.008	7.819	5.030
X <sub>Mg</sub>	0.346	0.283	0.624	0.596	0.586	0.606	0.581		0.424	0.277	0.855	0.631	
X <sub>Al</sub>			0.102	0.194	0.193	0.141	0.154						

gt(c) garnet core; gt(r) garnet rim; opx(i) orthopyroxene inclusion in garnet; opx(c) orthopyroxene core; opx(r) orthopyroxene rim; opx(2) M2 orthopyroxene; sp(i) spinel inclusion; sp(o) spinel in matrix

~0.9 GPa/~870 °C for the post-peak opx-sil-bt-bearing high-temperature mineral assemblage (M2) are consistent with its medium-pressure high-temperature stability field in the petrogenetic grid (Fig. 3). This suggests that if biotite and opx-sil-qtz are in paragenetic association, they cannot necessarily be used to indicate a UHT metamorphic condition.

## 5 Zircon U-Pb age dating

Zircon U-Pb analysis was conducted on an Agilent 7500a type LA-ICP-MS machine with a RESolution M50 type laser ablation system at State Key Laboratory of Isotope Geochemistry, Guangzhou Institute of Geochemistry, Chinese Academy of Sciences. Detailed analytical procedures have been reported previously [37, 38]. Zircons in the UHT metapelitic granulite are mainly euhedral and

long columnar crystals, and their CL images show no remarkable zoning (Fig. 4). Th/U ratios are larger than 0.1, and indicate that they are zircons formed during metamorphic recrystallization. The ages obtained from the analyses of 18 zircon grains are mostly between 260–280 Ma, with a concordant age of  $271 \pm 5$  Ma ( $n = 18$ , MSWD = 1.5) (Fig. 4). As this group of zircons formed during UHT metamorphism, the age should reflect the time when the Altay UHT metamorphic event occurred.

## 6 Geological significance

Through detailed petrographic observations and *P-T* estimates, in this paper we have firstly recognized the existence of gt-opx-sil-cd-bearing UHT metapelitic granulite near Kalasu of Altay. Orthopyroxene has a high-Al feature in composition, and its Al<sub>2</sub>O<sub>3</sub> content is as high as

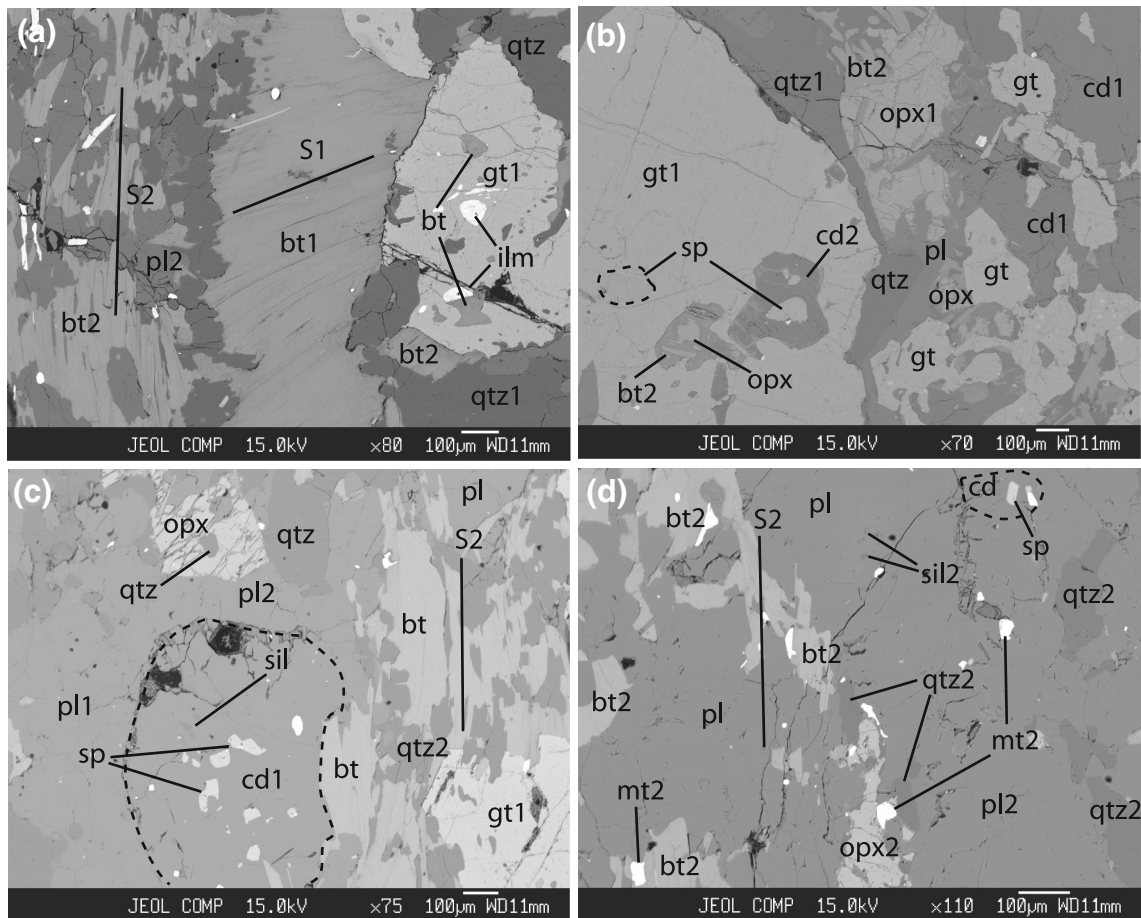


**Fig. 2** The Back Scattered Images (BSI) of the UHT metapelitic granulite in the Altay orogen. (a) two phases of gneissic foliation S1 and S2 defined by different orientation of biotite flakes, and garnet contains biotite and ilmenite inclusions; (b) garnet porphyroblast contains orthopyroxene and spinel inclusions, with retrograde biotite and cordierite around them, respectively; (c) cordierite contains spinel and sillimanite inclusions; (d) oriented M2 mineral assemblage opx-bt-sil-pl-qtz. Mineral abbreviations: *gt* garnet; *opx* orthopyroxene; *sil* sillimanite; *cd* cordierite; *sp* spinel; *bt* biotite; *pl* plagioclase; *ilm* ilmenite; *mt* magnetite; *qtz* quartz. 1 and 2 represent M1 and M2 mineral assemblages, respectively

8.7 wt%, indicating that its peak metamorphism reached UHT conditions (>900 °C). *P-T* estimates indicate that its peak metamorphic conditions are ~0.8 GPa/~960 °C, whilst *P-T* conditions of three different metamorphic stages define an anticlockwise *P-T* path of initial prograde up-pressure and heating and post-peak near isobaric cooling in the petrogenetic grid of the KFMASH model system [36] (Fig. 3). The anticlockwise *P-T* path of post-peak near isobaric cooling often reflects a tectonic process involving initial crustal compression immediately followed by extension, and this process is normally accompanied by intrusions of deep-derived magma or thinning of mantle lithosphere, which may provide an important heat source resulting in rapid heating of thickening crust [39]. Therefore, the anticlockwise *P-T* path of post-peak near isobaric cooling obtained in this study suggests that the Altay UHT metapelitic granulite might have formed in a tectonic setting involving intrusions of deep-derived magma and

accompanied by extensional heating of the lower crust. This is consistent with the conclusion derived by Wang et al. [18], namely the medium-low pressure high-temperature pelitic granulite formed in an extensional tectonic setting of high heat flow.

The above results are contrasting with the inference from the UHT (>900 °C) metapelitic granulite reported by Li et al. [34] from Wuqiagou in Fuyun County, namely they considered that the UHT metapelitic granulite had a clockwise *P-T* path of post-peak decompression that might be associated with oceanic crustal subduction and plate collision. Since the mineral assemblages and textural relations in the UHT metapelitic granulites from the two areas are very similar, and peak minerals contain early spinel and other mineral inclusions, indicating that pre-peak metamorphic stage is located in the medium-low pressure high-temperature stability field in the petrogenetic grid, the UHT metapelitic granulite at Wuqiagou thus

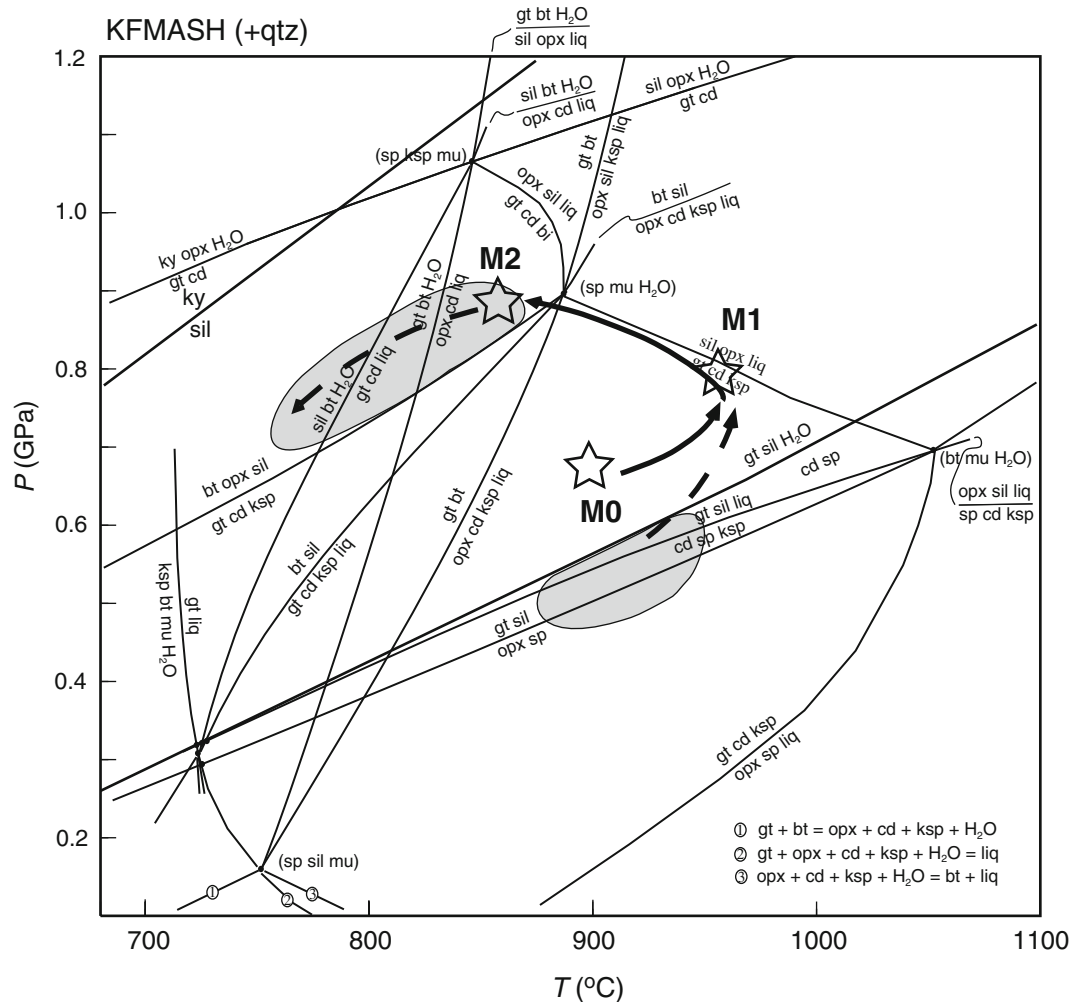


**Fig. 3**  $P$ - $T$  path of the UHT metapelitic granulite in the Altay orogen ( $P$ - $T$  petrogenetic grid in the KFMASH system after the reference [36]). Mineral abbreviations: *ky* kyanite; *mu* muscovite; *liq* melt; others are as in Fig. 2

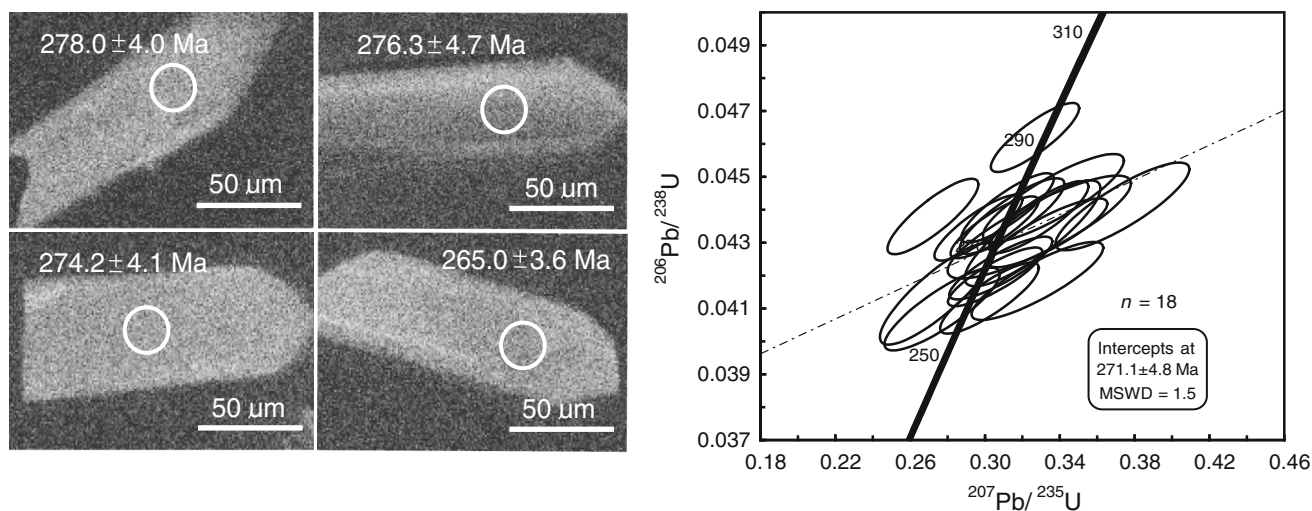


**Fig. 4** The CL images of zircons in the Altay UHT metapelitic granulite and U-Pb concordant diagram

might have actually experienced an anticlockwise  $P$ - $T$  history of post-peak near isobaric cooling similar to that of this study. Preliminary zircon U-Pb dating has been undertaken for the UHT metapelitic granulite from Kalasu, and the age data are mainly between 290–260 Ma, with a concordant age of  $271 \pm 5$  Ma (author's unpublished data), showing that the Altay UHT metamorphic event occurred in the Permian. Although Li et al. [34] also undertook zircon dating for the UHT metapelitic granulite at Wuqiagou, and thought that the UHT metamorphic event could form in the early Palaeozoic ( $\sim 499$  Ma), subsequent zircon age data ( $\sim 277$  Ma) support that the UHT metamorphic event may in fact have occurred in the Permian [40]. The timing of the granulite facies UHT metamorphic event is also compatible with the Permian metamorphic ages (270–280 Ma) of other medium-low pressure high-temperature granulites and gneisses in this orogenic belt [17, 18, 41, 42], suggesting that the UHT and high-temperature granulite facies metamorphic event in the Altay orogenic belt occurred in the Permian. As the UHT metapelitic granulite occurs as tectonic lenses within the medium-low pressure high-temperature pelitic granulites, this implies that the UHT metapelitic granulite might have been emplaced into the medium-low pressure high-temperature pelitic granulites through D2 tectonism.

The Altay Permian UHT metamorphic event confirmed in this study is consistent with the timing of the Permian Tarim mantle plume activity in Xinjiang ( $\sim 275$  Ma) [43], and is also compatible with the timing of the extensive Permian (280–260 Ma) mantle-derived genetic mafic to granitic magmatism formed in a post-orogenic or anorogenic extensional setting in the Altai region [29–33]. Thus, the Altay UHT metamorphism might be associated with magmatic intrusions and extensional heating of lower crust caused by Permian mantle plume activity. For instance, the post-orogenic or anorogenic Lamazhao granite and Fuyun granitic dykes were respectively intruded at 276 Ma and 275 Ma [26, 27], and they were derived from underplating of post-orogenic mantle-derived mafic magma [30], whilst the Kalatongke mafic intrusive complex (287 Ma) in Fuyun County was also considered to have formed during underplating of mantle-derived magma in a post-orogenic extensional setting [31]. All these support that a Permian mantle plume activity ( $\sim 275$  Ma) existed in the Altai region [29, 44]. Therefore, the Altay UHT metamorphic event could be closely associated with magmatic underplating and extensional heating of lower crust caused by the Permian Tarim mantle plume. This is not only consistent with the tectonic setting reflected from the anticlockwise  $P$ - $T$  path, but also compatible with the development of several gneissic thermal dome structures in the Altai region. Since the major phase of amphibolite facies metamorphism in the Altay orogenic belt occurred in the Devonian [15], and its corresponding arc-

continent collision formed the framework of this orogenic belt [11, 19], together with the time consistence of the UHT metamorphic event with the large Erqis deep fault or shear zone [33], it is suggested that this UHT metamorphism in the orogen could be an overprinting structural thermal metamorphic event caused by the Permian Tarim mantle plume activity.

**Acknowledgments** This work was supported by the National Basic Research Program of China (2011CB080901). We are very grateful to three anonymous reviewers for their helpful comments on the manuscript and to Dr. Georg F. Zellmer at Massey University for his polishing English of this paper. This is contribution No. IS-1835 from GIG-CAS.

## References

1. Harley SL (2004) Extending our understanding of ultrahigh temperature crustal metamorphism. *J Miner Petrol Sci* 99:140–158
2. Brown M (2007) Metamorphism, plate tectonics, and the supercontinent cycle. *Earth Sci Front* 14:1–18
3. Harley SL (2008) Refining the  $P$ - $T$  records of UHT crustal metamorphism. *J Metamorph Geol* 26:125–154
4. Tong L, Wilson CJL (2006) Tectonothermal evolution of the ultrahigh temperature metapelites in the Rauer Group, east Antarctica. *Precambrian Res* 149:1–20
5. Tsunogae T, Santosh M (2006) Spinel-sapphirine-quartz-bearing composite inclusion within garnet from an ultrahigh-temperature pelitic granulite: implications for metamorphic history and  $P$ - $T$  path. *Lithos* 92:524–536
6. Santosh M, Tsunogae T, Li JH et al (2007) Discovery of sapphirine-bearing Mg-Al granulites in the north China Craton: implications for Palaeoproterozoic ultrahigh-temperature metamorphism. *Gondwana Res* 11:263–285
7. Sengor AMC, Natal'in BA, Burtman VS (1993) Evolution of the Altaid tectonic collage and Palaeozoic crustal growth in Eurasia. *Nature* 54:117–137
8. Jahn BM (2004) The Central Asian Orogenic Belt and growth of the continental crust in the Phanerozoic. In: Malpas J, Fletcher CJN, Ali JR et al (eds). *Aspects of the Tectonic Evolution of China*. *Spec Publ* 226:73–100
9. Xiao W, Windley BF, Badarch G et al (2004) Palaeozoic accretion and convergent tectonics of the southern Altaids: implications for the growth of Central Asia. *J Geol Soc Lond* 161:339–342
10. He GQ, Han BF, Yue YJ et al (1990) Tectonic division and crustal evolution of Altay orogenic belt in China. *Geosci Xinjiang* 2:9–20
11. Windley BF, Kroner A, Guo J et al (2002) Neoproterozoic to Paleozoic geology of the Altai orogen, NW China: new zircon age data and tectonic evolution. *J Geol* 110:719–737
12. Zhuang YX (1994) The  $P$ - $T$ - $t$  evolution of metamorphism and development mechanism of the thermal-structural-gneiss domes in the Chinese Altaides. *Acta Geol Sin* 68:35–47
13. Zhang CG, Wei CJ, Qiu L (2004) Evolution of metamorphism and its geologic significance in Altaids, Xinjiang. *Xinjiang Geol* 22:16–23
14. Xu XC, Zheng CQ, Zhao QY (2005) Metamorphic types and crustal evolution of Hercynian orogenic belt in Altai region, Xinjiang. *J Jilin Univ* 35:7–11
15. Wei C, Clarke G, Tian W et al (2007) Transition of metamorphic series from the kyanite- to andalusite-types in the Altai orogen,

- Xinjiang, China: evidence from petrography and calculated KFMASH and KFMASH phase relations. *Lithos* 96:353–374
16. Li ZL, Chen HL, Yang SF et al (2004) Discovery of the basic granulite from the Altai area: evidence from mineralogy. *Acta Petrol Sin* 20:1445–1455
  17. Chen HL, Yang SF, Li ZL et al (2006) Zircon SHRIMP U-Pb chronology of the Fuyun basic granulite and its tectonic significance in the Altaid orogenic belt. *Acta Petrol Sin* 22:1351–1358
  18. Wang W, Wei CJ, Wang T et al (2009) Confirmation of pelitic granulite in the Altai orogen and its geological significance. *Chin Sci Bull* 54:918–923
  19. Wang T, Hong D, Jahn BM et al (2006) Timing, petrogenesis, and setting of Paleozoic synorogenic intrusions from the Altai Mountains, Northwest China: implications for the tectonic evolution of an accretionary orogen. *J Geol* 114:735–751
  20. Windley BF, Alexeiev D, Xiao W et al (2007) Tectonic models for accretion of the Central Asian Orogenic belt. *J Geol Soc Lond* 164:31–47
  21. Sun M, Long XP, Chai KD et al (2009) Early Palaeozoic ridge subduction in the Chinese Altai: insight from the abrupt change in zircon Hf isotopic compositions. *Sci China Ser D-Earth Sci* 39:935–948
  22. Jiang Y, Sun M, Zhao G et al (2010) The ~390 Ma high-*T* metamorphic event in the Chinese Altai: a consequence of ridge-subduction? *Am J Sci* 310:1421–1452
  23. Xiao WJ, Han CM, Yuan C et al (2006) Unique Carboniferous-Permian tectonic-metallogenic framework of northern Xinjiang (NW China): constraints for the tectonics of the southern Palaeoasian domain. *Acta Petrol Sin* 22:1062–1076
  24. Xiao W, Han C, Yuan C et al (2008) Middle Cambrian to Permian subduction-related accretionary orogenesis of Northern Xinjiang, NW China: implications for the tectonic evolution of central Asia. *J Asian Earth Sci* 32:102–117
  25. Sun M, Yuan C, Xiao W et al (2008) Zircon U-Pb and Hf isotopic study of gneissic rocks from the Chinese Altai: progressive accretionary history in the early to middle Paleozoic. *Chem Geol* 247:352–383
  26. Wang T, Hong DW, Tong Y et al (2005) Zircon U-Pb SHRIMP age and origin of post-orogenic Lamazhao granitic pluton from Altai orogen: its implications for vertical continental growth. *Acta Petrol Sin* 21:640–650
  27. Tong Y, Hong DW, Wang T et al (2006) TIMS U-Pb zircon ages of Fuyun post-orogenic linear granite plutons on the southern margin of Altai orogenic belt and their implications. *Acta Petrol Mineral* 25:85–89
  28. Zhou G, Zhang ZC, Luo SB et al (2007) Confirmation of high-temperature strongly peraluminous Mayin'ebo granites in the south margin of Altai, Xinjiang: age, geochemistry and tectonic implications. *Acta Petrol Sin* 23:1909–1920
  29. Zhang CL, Santosh M, Zou HB et al (2012) Revisiting the “Irtish tectonic belt”: implications for the Palaeozoic tectonic evolution of the Altai orogen. *J Asian Earth Sci* 52:117–133
  30. Tong Y, Wang T, Hong DW et al (2006) Pb isotopic composition of granitoids from the Altai orogen (China): evidence for mantle-derived origin and continental growth. *Acta Geol Sin* 80:517–528
  31. Han BF, Song B, Ji JQ et al (2004) SHRIMP zircon U-Pb age of mafic-ultramafic complex bearing copper and nickel and its geological significance in Kalatongke and East Huangshan, Xinjiang. *Chin Sci Bull* 49:2324–2328
  32. Cheng LH, Han BF (2006) Geochronology, geochemistry and Sr-Nd-Pb isotopic composition of mafic intrusive rocks in Wuqiagou area, north Xinjiang: constraints for mantle sources and deep processes. *Acta Petrol Sin* 22:1201–1214
  33. Briggs SM, Yin A, Manning CE et al (2007) Late Paleozoic tectonic evolution history of the Ertix Fault in the Chinese Altai and its implications for the development of the Central Asian Orogenic System. *GSA Bull* 119:944–960
  34. Li Z, Li Y, Chen H et al (2010) SHRIMP U-Pb zircon chronology of ultrahigh-temperature spinel-orthopyroxene-garnet granulite from south Altai orogenic belt, Northwestern China. *Isl Arc* 19:506–516
  35. Pattison DRM, Chacko T, Farquhar J et al (2003) Temperatures of granulite-facies metamorphism: constraints from experimental phase equilibria and thermobarometry corrected for retrograde exchange. *J Petrol* 44:867–900
  36. Tong L, Liu X, Wang Y et al (2014) Metamorphic *P-T* paths of metapelitic granulites from the Larsemann Hills, East Antarctica. *Lithos* 192:102–115
  37. Tu X, Zhang H, Deng W et al (2011) The application of RESolution laser ablation system in the in situ micro-area analysis of trace elements. *Geochimica* 40:83–98
  38. Liu YS, Hu ZC, Gao S et al (2008) In situ analysis of major and trace elements of anhydrous minerals by LA-ICP-MS without applying an internal standard. *Chem Geol* 257:34–43
  39. Sandiford M, Powell R (1991) Some remarks on high-temperature-low-pressure metamorphism in convergent orogens. *J Metamorph Geol* 9:333–340
  40. Li ZL, Li YQ, Wang HH et al (2012) Late Palaeozoic ultrahigh temperature metamorphism of the Altai and its evolution. 2012 national symposium on petrology and geodynamics (abst), p. 319
  41. Hu AQ, Wei GJ, Deng WF et al (2006) SHRIMP zircon U-Pb dating and its significance for gneisses from the southwest area to Qinghe County in the Altai, China. *Acta Petrol Sin* 22:1–10
  42. Zheng CQ, Xu XC, Kato T et al (2007) Permian CHIME ages of monazites for the kyanite-sillimanite type metamorphic belt in Chonghuer area, Altai, Xinjiang and their geological implications. *Geol J Chin Univ* 13:566–573
  43. Zhang CL, Li ZX, Li XH et al (2010) A Permian large igneous province in Tarim and Central Asian orogenic belt, NW China: results of a ca. 275 Ma mantle plume? *GSA Bull* 122:2020–2040
  44. Pirajno F, Mao J, Zhang ZC et al (2008) The association of mafic-ultramafic intrusions and A-type magmatism in the Tian Shan and Altai orogens, NW China: implications for geodynamic evolution and potential for the discovery of new ore deposits. *J Asian Earth Sci* 32:165–183